A two-stage R2 indicator based evolutionary algorithm for many-objective optimization

Li, Fei; Cheng, Ran; Liu, Jianchang; Jin, Yaochu

DOI:
10.1016/j.asoc.2018.02.048

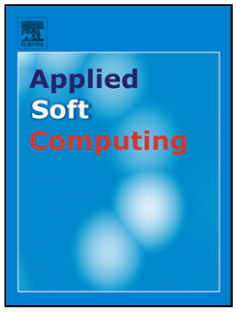

Title: A Two-Stage R2 Indicator Based Evolutionary Algorithm for Many-Objective Optimization

Author: Fei Li Ran Cheng Jianchang Liu Yaochu Jin

PII: S1568-4946(18)30107-8
DOI: https://doi.org/doi:10.1016/j.asoc.2018.02.048
Reference: ASOC 4740

To appear in: *Applied Soft Computing*

Received date: 14-9-2017
Revised date: 8-2-2018
Accepted date: 22-2-2018

Please cite this article as: Fei Li, Ran Cheng, Jianchang Liu, Yaochu Jin, A Two-Stage R2 Indicator Based Evolutionary Algorithm for Many-Objective Optimization, *<![CDATA[Applied Soft Computing Journal]]>* (2018), https://doi.org/10.1016/j.asoc.2018.02.048

Highlights

- A two-stage selection strategy has been proposed on the basis of both the R2 indicator and the reference vector guided objective space partition
- An R2 indicator based achievement scalarizing function has been designed for the primary selection
- A reference vector guided secondary selection has been adopted for objective space partition
- An evolutionary algorithm based on the two-stage selection strategy has been developed for many-objective optimization
- Experimental results demonstrate the competitive performance of the proposed evolutionary algorithm in comparison with some state-of-the-art algorithms for many-objective optimization

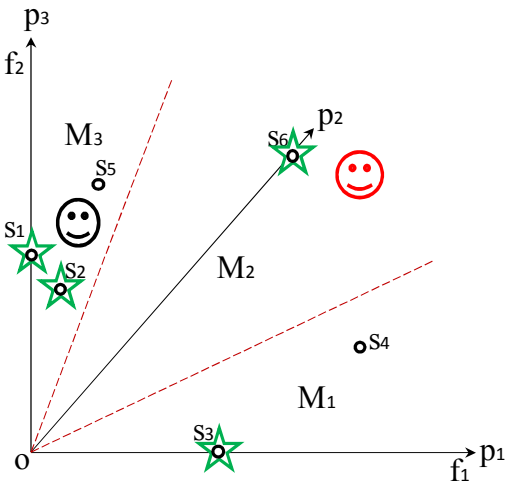

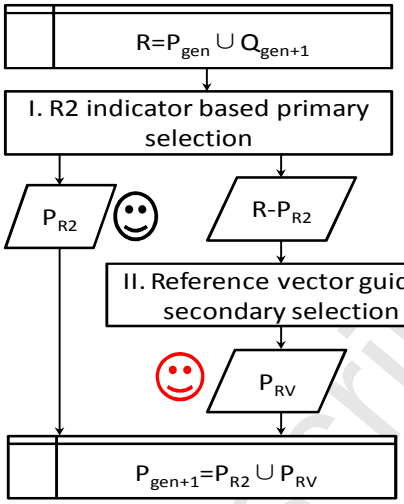

A Two-Stage R2 Indicator Based Evolutionary Algorithm for Many-Objective Optimization

Fei Li[a], Ran Cheng[b,*], Jianchang Liu[a], Yaochu Jin[c,d]

[a] *Department of Information Science and Engineering, Northeastern University, Shenyang 110819, P. R. China*
[b] *CERCIA Group, School of Computer Science, University of Birmingham, United Kingdom, B15 2TT*
[c] *Department of Computing, University of Surrey, Guildford, Surrey, GU2 7XH, United Kingdom*
[d] *College of Information Sciences and Technology, Donghua University, Shanghai 201620, P. R. China*

Abstract

R2 indicator based multi-objective evolutionary algorithms (R2-MOEAs) have achieved promising performance on traditional multi-objective optimization problems (MOPs) with two and three objectives, but still cannot well handle many-objective optimization problems (MaOPs) with more than three objectives. To address this issue, this paper proposes a two-stage R2 indicator based evolutionary algorithm (TS-R2EA) for many-objective optimization. In the proposed TS-R2EA, we first adopt an R2 indicator based achievement scalarizing function for the primary selection. In addition, by taking advantage of the reference vector guided objective space partition approach in diversity management for many-objective optimization, the secondary selection strategy is further applied. Such a two-stage selection strategy is expected to achieve a balance between convergence and diversity. Extensive experiments are conducted on a variety of benchmark test problems, and the experimental results demonstrate that the proposed algorithm has competitive performance in comparison with several tailored algorithms for many-objective optimization.

Keywords: R2 indicator, reference vector, two-stage selection strategy,

*Corresponding author.
Email addresses: lanceleeneu@126.com (Fei Li), ranchengcn@gmail.com (Ran Cheng), liujianchang@ise.neu.edu.cn (Jianchang Liu), yaochu.jin@surrey.ac.uk (Yaochu Jin)

many-objective optimization, evolutionary algorithm.

1. Introduction

A multi-objective optimization problem (MOP), which involves more than one conflicting objectives to be optimized simultaneously, can be formulated as follows:

$$\begin{aligned} &min \qquad F(x) = (f_1(x), f_2(x), ..., f_m(x)) \\ &s.t. \quad x \in \Omega \end{aligned} \tag{1}$$

where $x = (x_1, x_2, ..., x_n)$ is the decision vector, n is the dimension of decision space, Ω is the decision space, m is the number of objectives, $F(x)$ is the m dimensional objective vector and $f_i(x)$ is the ith objective to be optimized.

A solution x^1 in the decision space is said to dominate another solution x^2 ($x^1 \prec x^2$) if and only if $f_i(x^1) \leq f_i(x^2)$ for every $i \in \{1, ..., m\}$, and $f_j(x^1) < f_j(x^2)$ for at least one index $j \in \{1, ..., m\}$. A solution x^* is a Pareto optimal solution if there is no other solution $x \in \Omega$ such that $x \prec x^*$, and correspondingly, $F(x^*)$ is called a Pareto optimal vector. Due to the conflicting nature of MOPs, any improvement of a Pareto optimal vector in one objective will deteriorate at least one other objective. A set of Pareto optimal vectors in objective space is called Pareto front (PF) while the corresponding image in decision space is known as Pareto set (PS) [1, 2].

Since population based metaheuristics such as evolutionary algorithms (EAs) can obtain a set of candidate solutions in a single run, the multi-objective evolutionary algorithms (MOEAs) have witnessed a rapid development during the last two decades [3]. Nevertheless, although most MOEAs perform well on MOPs with two and three objectives, they are confronted with various issues when applied to many-objective optimization problems (MaOPs) with more than three objectives. In recent years, the development of MOEAs for solving MaOPs has attracted increasing interest in the literature [4]. As one major reason behind the failure of traditional MOEAs in solving MaOPs, the phenomenon called dominance resistance causes severe loss of convergence pressure

towards the Pareto front [5]. In order to enhance the performance of MOEAs in many-objective optimization, various approaches have been proposed during the last few years. They can be divided into three categories.

The first category is still Pareto dominance based MOEAs, where the basic idea is to enhance the selection pressure by applying various modified dominance relations or novel diversity management strategies. Some representative modified dominance relations include the fuzzy dominance [6, 7], grid dominance [8] and preference-inspired method [9]. Instead of applying modified dominance relations to enhance convergence in an explicit manner, some work tries to implicitly improve the convergence quality via diversity management. For example, Li *et al*. proposed a modified crowding distance diversity criterion for Pareto dominance based MOEAs, namely, the shift-based density estimation (SDE) strategy [10]. Recently, Zhang *et al*. proposed a knee point-driven evolutionary algorithm for many-objective optimization, namely, KnEA [11].

The second category is the decomposition based evolutionary algorithms. The most representative MOEAs based on decomposition are C-MOGA [12], MOEA/D [13] and MOEA/D-M2M [14]. Recently, some MOEAs based on both dominance and decomposition have also been proposed [15, 16, 17].

The third category is known as the indicator based MOEAs. As the most prevalent performance indicator in the literature, the hypervolume indicator is strictly monotonic with regard to Pareto dominance [18, 19], and the representative MOEAs based on it include the SMS-EMOA [20] and the HypE [21]. More recently, an evolutionary algorithm based on both Pareto dominance and performance indicator (Two_Arch2) has also been proposed [22]. Although hypervolume indicator based MOEAs are able to transform an MOP/MaOP into an SOP, they suffer from a serious curse of dimensionality due to the exponentially increasing computational cost of the hypervolume calculation.

Apart from the hypervolume indicator, there are also some other performance indicators in the literature such as GD [23], $IGD+$ [24, 25] and Δ_p [26]. Recently, the R2 indicator, which strikes a comprehensive balance between convergence and diversity, has attracted increasing interest [27]. Given a set of

reference vectors, the R2 indicator can be regarded as the mutual preference based on the population contribution to each reference vector by ranking the population. There are some desirable properties such as weak monotonicity to the Pareto dominance and low computational complexity which make it a viable candidate to be embedded into indicator based MOEAs, often known as the R2-MOEAs [27, 28, 29].

Compared to other existing MOEAs, the R2-MOEAs have some advantages, e.g., the scalability in terms of the number of objectives [30], robustness to noisy problems [31], simple hybridization with other metaheuristics [32, 33], etc. Generally, an R2-MOEA consists of three main components: reference vector generation [34], scalarizing function formulation [35] and nadir point updated strategy [36]. Firstly, systematic sampling methods such as DBEA [37] and RVEA [38] are commonly used to generate reference vectors for an R2-MOEA. Secondly, a variety of scalarizing methods are also available, including the prominent examples of weighted sum, Tchebycheff and augmented weighted Tchebycheff method [35]. Thirdly, the most commonly used nadir point updated strategies include fixed nadir point, adaptive nadir point adjustment and record data structure nadir point adjustment [36].

Although R2-MOEAs have been successfully applied to solving bi-/three-objective MOPs [39], as pointed in [27], research on R2-MOEAs for solving MaOPs is still in the infancy. Inspired by the recently proposed reference vector guided evolutionary algorithm (RVEA) [38], we propose an enhanced R2 indicator based MOEA, known as the TS-R2EA, where the main motivation is to take the advantages of both R2 indicator and reference vector guided selection strategy in RVEA to strike a good balance between convergence and diversity for many-objective optimization. To this end, a two-stage selection strategy is proposed, where the primary and secondary selections are based on the R2 indicator and guided by reference vectors, respectively. The primary selection first ranks the population based on the R2 indicator, and the candidate solutions which are located in the first rank will be selected. Then, the secondary selection is guided by a set of reference vectors, where the remaining candidate

solutions in the partitioned subspaces are further selected to maintain a proper population diversity.

The rest of this paper is organized as follows. Section 2 introduces the background and motivation of this work. Section 3 describes the proposed TS-R2EA for many-objective optimization in detail. Section 4 presents test problems, performance indicators and algorithm settings used for the empirical studies. Section 5 provides the extensive experimental results and discussions. Finally, conclusions and future work are given in Section 6.

2. Background and Motivation

In this section, we first provide some basic knowledge about the R2 indicator. Then, we briefly introduce the general mechanism of RVEA [38] and R2-MOEAs [27], which are directly related to the proposed TS-R2EA. Finally, the motivation of this work is given.

2.1. R2 Indicator

The R2 indicator is designed on the basis of utility functions which map the candidate solutions from the objective space into utility space for performance assessment [27, 28]. Among various utility functions, the most widely used ones are the weighted sum (WS) [40] and the Tchebycheff (TCH) [30] utility function, both of which are well suited for solving bi-/three-objective optimization problems [36]. However, their performance deteriorates rapidly as the number of objectives increases [30]. As suggested in some recent studies [36], an achievement scalarizing utility function (ASF) is more suitable for solving MaOPs. Therefore, we decided to incorporate the ASF into the R2 indicator in this work:

$$ASF(\vec{a}, z^*, \vec{\lambda}) = \max_{i \in \{1,\ldots,m\}} \left\{ \frac{1}{\lambda_i} |z_i^* - a_i| \right\}, \tag{2}$$

where $\vec{a}$ denotes a candidate solution, z^* is the ideal point which minimizes all objective functions, and each ith component is defined as $z_i^* = \min_{\vec{a}} f_i(\vec{a})$,

$\vec{\lambda} = (\lambda_1, ..., \lambda_m)$ represents a user specified reference vector, $\lambda_i \geq 0$ for all $i \in \{1, ..., m\}$, m is the number of objectives.

Given an approximation set A, a set of reference vectors V, and the utility function u, the unary R2 indicator can be calculated as follows:

$$R2(A, V) = \frac{1}{|V|} \sum_{\vec{\lambda} \in V} \min_{\vec{a} \in A} \left\{ u_{\vec{\lambda}}(\vec{a}) \right\}. \tag{3}$$

After properly choosing the utility function as given in Eq. (2), we put the ASF formula into Eq. (3). Finally, we can calculate the R2 with respect to the candidate solution set A as follows:

$$R2(A, V) = \frac{1}{|V|} \sum_{\vec{\lambda} \in V} \min_{\vec{a} \in A} \left\{ \max_{i \in \{1,...,m\}} \{ \frac{1}{\lambda_i} |z_i^* - a_i| \} \right\}. \tag{4}$$

Correspondingly, the contribution of a candidate solution $\vec{a} \in A$ to the R2 indicator can be calculated as:

$$C_{R2}(\vec{a}, A, V) = R2(A, V) - R2(A \backslash \{\vec{a}\}, V). \tag{5}$$

2.2. RVEA

The basic idea of RVEA [38] is to guide the search of an MOEA using a set of reference vectors by partitioning the objective space into a number of subspaces. In each generation of RVEA, at most one candidate solution can be selected in each subspace according to the selection criterion known as the angle penalized distance (APD). To deal with scaled problems where the objective functions are not well normalized, RVEA adopts a reference vector adaptation strategy to dynamically adjust the distribution of the reference vectors, such that a uniform distribution of the candidate solutions can be guaranteed. As reported in [38], RVEA has a promising performance on a variety of MaOPs in comparison with some state-of-the-art MOEAs for many-objective optimization.

2.3. R2-MOEAs

Similar to RVEA, R2-MOEA first specifies a set of reference vectors that uniformly spread over the objective space. In each generation of R2-MOEAs,

a non-dominated sorting procedure is first applied to divide the combined population into several ranks. Candidate solutions in the first-rank front have the highest priority to be selected. The second-rank candidate solutions will be identified in the same manner from the remaining candidate solutions. The procedure will continue until all the candidate solutions have been ranked. As a consequence, the candidate solutions in the last acceptable front are selected using R2 contributions as given in Eq. (5). It is worth noting that the number of candidate solutions to be selected in each generation is always equal to the number of reference vectors in R2-MOEAs, while in RVEA, due to the fact that some subspaces can be empty, it is possible that the number of selected candidate solutions is smaller than the number of reference vectors.

2.4. Motivation for TS-R2EA

It has been widely reported that the R2 indicator can well balance convergence and diversity when solving bi-/three-objective MOPs [39]. However, as presented in some recent work [36], its performance substantially deteriorates when R2-MOEAs are applied to the optimization of MaOPs. In the proposed TS-R2EA, we are motivated to enhance the diversity management by taking advantage of the reference vector guided selection strategy adopted in the recently proposed RVEA [38], such that a better balance between diversity and convergence can be achieved in the R2 indicator based evolutionary many-objective optimizer.

In order to have a clear understanding of selection strategies in traditional R2-MOEAs and the proposed TS-R2EA, we provide an illustrative example in Fig. 1, where $\{s1, s2, s3, s4, s5, s6\}$ are the combined candidate solutions, and $\{\lambda 1, \lambda 2, \lambda 3\}$ and $\{M_1, M_2, M_3\}$ are a set of reference vectors and the corresponding subspaces respectively. The traditional R2-MOEAs only select candidate solutions $\{s1, s2, s3\}$, although $s6$ in the subspace $M2$ has a significant contribution to the population diversity. Fortunately, RVEA selects candidate solutions $\{s1, s6, s3\}$, where the candidate solution $s6$ is crucial to the diversity maintenance. Thus, the two-stage selection strategy in TS-R2EA

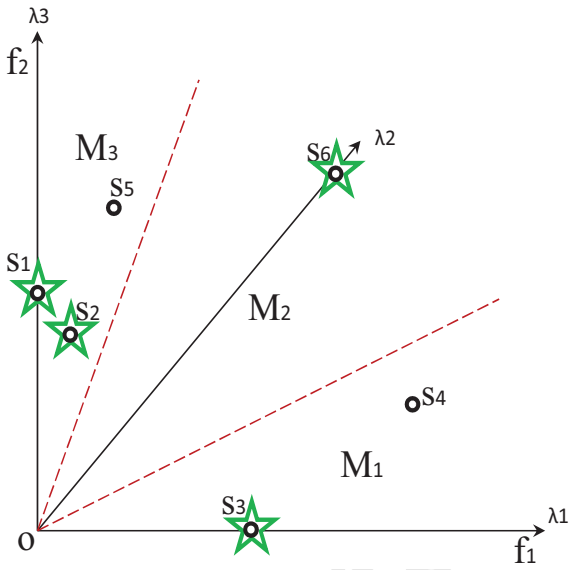

Figure 1: Illustrations of the proposed TS-R2EA. $\{s1, s2, s3, s4, s5, s6\}$ are the combined candidate solutions. $\{\lambda 1, \lambda 2, \lambda 3\}$ are a set of reference vectors, where the corresponding subspaces are $\{M_1, M_2, M_3\}$.

not only selects the candidate solutions in the first rank, namely $\{s1, s2, s3\}$, but also selects $s6$ according to the reference vector guided selection strategy. Consequently, the two-stage selection strategy is able to strike a good balance between convergence and diversity.

3. Proposed Algorithm: TS-R2EA

3.1. Framework of TS-R2EA

Essentially, the proposed TS-R2EA is still an elitist MOEA based on the R2 indicator. However, the main difference between TS-R2EA and MOMBI-II [36] lies in the fact that the reference vector guided secondary selection strategy is adopted.

The main framework of the proposed TS-R2EA is presented in Algorithm 1 and Fig. 2. Firstly, a number of N candidate solutions and reference vectors are

Algorithm 1 TS-R2EA Main Loop

1: Initialization (P_0, V_0)
2: $gen \leftarrow 0$
3: **repeat**
4: $\quad Q_{gen+1} \leftarrow$ Reproduction (P_{gen})
5: $\quad P_{gen+1} \leftarrow$ TS-R2EA-Selection $(P_{gen} \cup Q_{gen+1})$
6: $\quad gen \leftarrow gen + 1$
7: **until** Termination condition satisfied
8: Return P

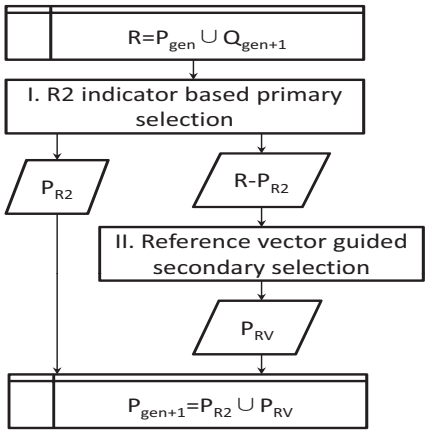

Figure 2: Illustration of the main loop of TS-R2EA. P_{gen} and Q_{gen+1} are the parent population and the offspring population respectively. P_{R2} and P_{RV} are the selected candidate solutions obtained by adopting the two-stage selection strategies.

initialized in P_0 and V_0 respectively. In the main loop, the offspring population is first generated using genetic operators such as the simulated binary crossover (SBX) [41] and the polynomial mutation (PM) [42]. Then, the TS-R2EA selection strategy is used to select a new population for the next generation. Specifically, the TS-R2EA selection consists of two components in Fig. 2: P_{R2} and P_{RV}, which are selected by adopting the R2 indicator based primary selection approach and the reference vector guided secondary selection method. In the following subsections, each main component in TS-R2EA will be explained

step-by-step.

3.2. Initialization Procedure

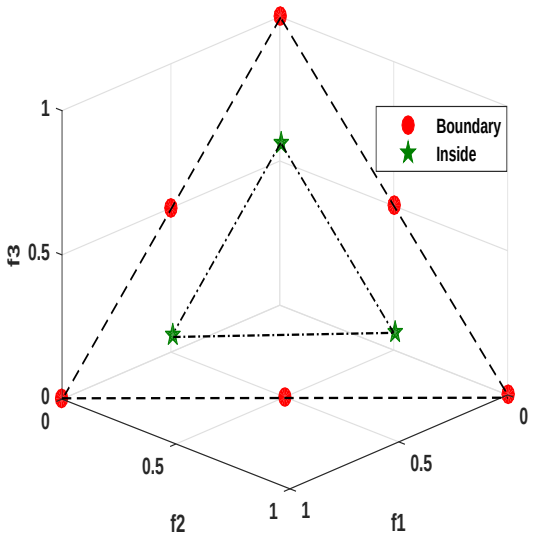

Figure 3: Illustration of the two-layered reference points (with six points on the boundary layer ($H1 = 2$) and three points on the inside layer ($H2 = 1$)).

The initialization procedure of TS-R2EA involves two aspects: the initial parent population P_0 and a set of reference vectors V_0. More specifically, P_0 is randomly sampled from the decision space via a uniform distribution. What follows is to generate a set of uniformly distributed reference vectors. To be specific, a set of uniformly distributed reference points is first generated on a normalized hyperplane using the canonical simplex lattice design method [43]. A number of $N = C_{H+m-1}^{m-1}$ reference points, with a uniform spacing of $1/H$, where C is the Combinatorial operation and $H > 0$ is the number of divisions considered along each objective coordinate, are sampled on the simplex for any number of objectives. As illustrated in Fig. 3, we adopt two layers of reference points with small values of H, where $H1$ is used for the boundary layer and $H2$ is used for the inside layer. Thus, a number of $N = C_{H1+m-1}^{m-1} + C_{H2+m-1}^{m-1}$ reference

points are generated. The corresponding reference vector V_0 is then obtained by projecting the reference points from the hyperplane to the hypersphere.

3.3. TS-R2EA Selection Strategy

In principle, the offspring population Q_{gen+1} can be generated by any genetic operator. In this paper, we use the simulated binary crossover (SBX) [41] and the polynomial mutation (PM) [42]. After the generation of the offspring population, it is combined with the parent population P_{gen} to undergo the selection strategy as presented in Algorithm 2. R is the combined population which combines P_{gen} and Q_{gen+1}. FR is the corresponding objective values of R. FR is translated into $\overline{FR}$ by subtracting the ideal point z^* at Step 2 in Algorithm 2. Then, the two-stage selection procedure will be performed.

Firstly, in the R2 indicator based primary selection as illustrated from Step 3 to Step 5 in Algorithm 2, the R2 contribution of each candidate solution is calculated using Algorithm 3, and as a consequence, candidate solutions with non-zero contributions are selected.

Secondly, the objective space is partitioned into a number of subspaces using Algorithm 4. The remaining candidate solutions that have no contribution to the R2 indicator will further undergo the reference vector guided secondary selection as illustrated from Step 6 to Step 20 in Algorithm 2. More specifically, the angle penalized distance (APD) [38] is used as the selection criterion here:

$$APD = (1 + m \cdot (\frac{gen}{Gen})^{\alpha} \cdot (\frac{\beta}{\gamma})) \cdot \|FS\|, \tag{6}$$

where m is the number of objectives, α is a user defined parameter to balance the convergence and diversity, β is the acute angle between the candidate solutions and the corresponding reference vector, gen and Gen are the current and maximal iterations respectively, γ is the smallest angle value between reference vector and the other reference vectors in the current iteration, $\|FS\|$ denotes the convergence criterion.

Consequently, the candidate solutions selected via the two-stage selection strategy, namely P_{R2} and P_{RV}, are combined to be the parent population P_{gen+1}

Algorithm 2 TS-R2EA Selection Procedure

Input: The parent population P_{gen}, the offspring population Q_{gen+1};

Output: The selected population P_{gen+1};

$R \leftarrow P_{gen} \cup Q_{gen+1}$, $FR \leftarrow F(P_{gen}) \cup F(Q_{gen+1})$;
$\overline{FR} \leftarrow$ Translate objective values of FR by subtracting the ideal point z^*;
/* R2 indicator based primary selection */
$Contr \leftarrow$ R2 contribution $(\overline{FR}, V)$ in Algorithm 3;
$P_{R2} \leftarrow$ Select the candidate solutions where $Contr$ is larger than 0;
/* Reference vector guided secondary selection */
$M \leftarrow OSP(R, \overline{FR}, V)$ in Algorithm 4;
$M(P_{R2}) \leftarrow \emptyset$; /* Delete subspaces and their solutions occupied by P_{R2} */
for $i \leftarrow \{1, ..., |V|\}$ **do**
  if subspace $M(i)$ is not empty **then**
    $S \leftarrow M(i)$, $FS \leftarrow \overline{FR}(S)$;
    if the size of S is more than one **then**
      Calculate the acute angle β;
      Calculate the convergence criterion $\|FS\|$;
      Calculate the APD value using Eq. (6);
      /*Solution with the minimum APD value survives*/
      $P_{RV} \leftarrow P_{RV} \cup S(\min(APD))$;
    end
  end
end
/* Population combination */
$P_{gen+1} \leftarrow P_{R2} \cup P_{RV}$;
if $\mod(gen, f_r * Gen) \leftarrow 0$ **then**
  $VV \leftarrow V_0 * (z^{max} - z^*)$;
  $V \leftarrow \frac{VV}{\|VV\|}$;/* Reference vector adaptation */
end

Algorithm 3 Calculation of R2 contribution

Input: The normalized objective values $\overline{FR}$, a set of reference vectors V;

Output: The R2 contribution $Contr$;

1: **for** each reference vector $k \leftarrow \{1, ..., |V|\}$ **do**
2: **for** each candidate solution $j \leftarrow \{1, ..., |\overline{FR}|\}$ **do**
3: /∗Calculate the utility function value∗/
4: $ASF(k, j) \leftarrow \max_{i \in \{1,...,m\}} \left\{ \frac{|\overline{FR}_i(j)|}{\lambda_i(k)} \right\}$;
5: **end**
6: /∗Obtain the $minASF$ and its corresponding $Index$ in the $\overline{FR}$ ∗/
7: $(minASF, Index) \leftarrow$ Find the minimum value of ASF and its $Index$;
8: /∗Calculate the R2 contribution of each individual∗/
9: $Contr \leftarrow$ Add the $minASF$ together as each individual R2 contribution;
10: **end**
11: **Return:** $Contr$

of the next generation at Step 22 in Algorithm 2. After obtaining the population P_{gen+1}, we calculate the maximal objective values of P_{gen+1}, namely z^{max}. Meanwhile, z^* represents the minimal objective values calculated from P_{gen+1}. Then, we adopt the reference vector adaptation method according to the ranges of the objective values at Step 24 and Step 25.

In the following, we will further detail the R2 contribution calculation procedure and the reference vector guided objective space partition approach adopted in the primary and secondary selections respectively.

3.3.1. R2 indicator based primary selection

There are various potential choices of existing utility functions for the R2 indicator, e.g., the weighted sum, the weighted Tchebycheff functions or the hybridization of both. As for TS-R2EA, we choose the achievement scalarizing function (ASF) metric [36] as the utility function to calculate the R2 contribution of each candidate solution.

Traditional utility functions only calculate the indicator values of the can-

Algorithm 4 Reference vector guided objective space partition (OSP)

Input: The population R and the normalized objective values $\overline{FR}$, a set of reference vectors V;

Output: The objective subspace set M;

for each candidate solution $i \leftarrow \{1, ..., |\overline{FR}|\}$ **do**
  for each reference vector $j \leftarrow \{1, ..., |V|\}$ **do**
    /*Cosine similarity between $\overline{FR}$ and V */;
    $\cos \delta_{i,j} \leftarrow \frac{\overline{FR}(i) \cdot \lambda(j)}{\|\overline{FR}(i)\|}$;
  end
end
/*Find the closest subspace*/
for each candidate solution $i \leftarrow \{1, ..., |\overline{FR}|\}$ **do**
  $c \leftarrow \arg \max_{j \in \{1,...,|V|\}} \cos \delta_{i,j}$;
  /*Add R into the nearest subspace M */
  $M(c) \leftarrow M(c) \bigcup \{R(i)\}$;
end
Return: M

didate solutions with respect to each reference vector. By contrast, the R2 indicator not only considers the utility function value towards each reference vector but also adds these values together as the R2 contribution of each candidate solution. Algorithm 3 describes the calculation of R2 contribution $Contr$ via introducing the achievement scalarizing utility function. We obtain the ASF value of $\overline{FR}$ corresponding to each reference vector from Step 2 to Step 5 in Algorithm 3. For each reference vector, the best candidate solution and its corresponding ASF value is preserved, while the ASF value of the other candidate solutions to this reference vector will be 0 at Step 6 and 7. After getting the ASF value of each candidate solution with respect to each reference vector, we sum up the contribution values of each candidate solution as its R2 contribution $Contr$ at Step 8 and 9.

Once the R2 contribution values of the candidate solutions are obtained using Algorithm 3, the primary selection method based on the R2 indicator from Step 4 to Step 5 in Algorithm 2 can be operated. Consequently, the candidate solutions having non-zero R2 contribution values are selected and preserved in P_{R2}.

Table 1: Illustration of the R2 contribution calculation in Fig. 1. $(s1, s2, s3, s4, s5, s6)$ are candidate solutions, $(\lambda1, \lambda2, \lambda3)$ are reference vectors, $Contr$ denotes the R2 contribution.

$S \setminus V$	$\lambda1$(1,0.001)	$\lambda2$(0.5,0.5)	$\lambda3$(0.001,1)	$Contr$
$s1$(0,1)	1000	2	1	*1*
$s2$(0.2,0.8)	800	1.6	200	*1.6*
$s3$(1,0)	1	2	1000	*1*
$s4$(1.8,0.5)	500	3.6	1800	0
$s5$(0.4,1.2)	1200	2.4	1200	0
$s6$(1.5,1.5)	1500	3	1500	0

In order to better understand the R2 indicator based primary selection scheme, we present an illustrative example. Given a set of reference vectors $V = \{\lambda1, \lambda2, \lambda3\}$ and a set of candidate solutions $S = \{s1, ..., s6\}$ in Fig. 1, Table 1 summarizes the R2 indicator contribution values in terms of the achieve-

ment scalarizing utility function. The best utility function values and the best R2 contribution values of the candidate solutions are in gray background in Table 1. According to the R2 contribution values, to be specific, $\{s1, s2, s3\}$ will be selected by the primary selection strategy, whereas the remaining candidate solutions $\{s4, s5, s6\}$ will be discarded. However, as will be presented in the following, since $s6$ is crucial to the population diversity, it will be further preserved by the secondary selection.

3.3.2. Reference vector guided secondary selection

The candidate solutions with promising convergence are preserved by the R2 indicator based primary selection. However, how to maintain a good balance between convergence and diversity is crucial to the performance of the proposed TS-R2EA. Therefore, it is expected that the secondary selection is capable of well managing the population diversity. As reported in [38], the reference vector guided objective space partition is particularly useful for diversity management in many-objective optimization. To be specific, Algorithm 4 first divides the objective space into a number of $|V|$ subspaces $M_1, M_2, ..., M_V$ by associating each candidate solution with its closest reference vector. To determine the spacial relationship between the candidate solutions and the reference vectors, the acute angles between them are calculated. In this way, each candidate solution is allocated to a subspace M_j if and only if the acute angle between this candidate solution and $\lambda(j)$ is minimal (i.e., the cosine value is maximal) among all the reference vectors.

After associating each candidate solution with its closest reference vector, we delete subspaces occupied by P_{R2} and their corresponding candidate solutions at Step 8 in Algorithm 2. Once the objective space is divided into a group of subspaces $M_1, M_2, ..., M_V$, selection is performed inside each subgroup independently from Step 9 to Step 20 in Algorithm 2. More specifically, if a subspace M_i is non-empty, we adopt the APD metric to select the solution which has the best APD value. Finally, all selected candidate solutions from the non-empty subspaces will be merged into P_{RV}.

3.4. Computational Complexity of the Proposed TS-R2EA

In this subsection, we analyze the computational complexity of the proposed TS-R2EA. The main computational cost results from the two-stage selection strategy apart from the variation operation. As shown in Algorithm 2, the two-stage selection strategy consists of four main components: the objective value translation, the primary selection, the secondary selection and the reference vector adaptation procedure.

The time complexity of the objective value translation is $O(m|R|)$, where m is the number of objectives and $|R|$ is the size of candidate solution set. Then, the computational cost of the primary selection strategy is $O(|R||V|(log|R|+m))$ as shown in Algorithm 3, where $|V|$ is the size of reference vector set. As for the secondary selection strategy [38] in Algorithm 2, the time complexity for the objective space partition strategy is $O(m|R|^2)$. The cost of calculating the APD and the corresponding selection are $O(m|R|^2)$ and $O(|R|^2)$ in the worst case, respectively. In addition, the computational complexity for the reference vector adaptation procedure is $O(m|R|/(f_r * Gen))$, where f_r and Gen denote the frequency to employ the reference vector adaptation strategy and the maximal number of generations, respectively. Therefore, the overall complexity of the proposed TS-R2EA at each generation is $O(m|R|^2)$.

3.5. Discussions

It should be noted that, although the proposed TS-R2EA is partially inspired by MOMBI-II and RVEA, there are also some significant differences which can be summarized as follows.

As for TS-R2EA and MOMBI-II, both of them employ the R2 indicator to perform selection without adopting any Pareto dominance method. However, there are two major differences between the two algorithms. Firstly, TS-R2EA adopts a reference vector guided secondary selection strategy to maintain the diversity while MOMBI-II only adopts the fast R2 ranking strategy for selection. Secondly, to handle badly-scaled Pareto fronts, TS-R2EA adopts an adaptation

strategy to normalize the reference vectors, while MOMBI-II adopts the normalization of the objective values using the historical information. For example, TS-R2EA preserves $\{s1, s2, s3, s6\}$ while MOMBI-II only selects $\{s1, s2, s3\}$ as shown in Fig. 1, despite that $s6$ is crucial to the population diversity.

As for TS-R2EA and RVEA, both of them adopt a reference vector guided selection strategy for diversity management in the high-dimensional objective space. Nevertheless, TS-R2EA performs a two-stage selection strategy, where the primary selection is based on the R2 indicator and the secondary selection is based on the reference vector guided strategy; by contrast, the selection strategy in RVEA is merely guided by reference vectors. To be specific, RVEA only selects $\{s1, s3, s6\}$ according to the reference vector guided objective space partition strategy and the APD metric as shown in Fig. 1. However, the candidate solution $s2$, which has an important contribution to the population convergence, will be discarded by RVEA.

In summary, our major motivation is to exploit the merits of both R2 indicator and reference vector guided selection approaches for balancing convergence and diversity in evolutionary many-objective optimization. In the next section, the performance of our proposed TS-R2EA will be assessed on a set of benchmark test problems in comparison with some other tailored algorithms for many-objective optimization.

4. Experimental Study

This section presents an experimental setup for investigating the performance of TS-R2EA. First, a set of benchmark test problems used in the experiments are given. Then, we introduce performance indicators to assess the convergence and diversity of these MOEAs. Finally, the experimental settings adopted in this study are provided.

4.1. Benchmark Test Problems

Empirical experiments are conducted on two well-known test suites for many-objective optimization, i.e., the Deb-Thiele-Laumanns-Zitzler (DTLZ) [44] and

the Walking-Fish-Group (WFG) [45] test suites. These test suites can be scaled to have any number of objectives. For each test problem, the number of objectives is varied from three to fifteen, i.e., $m \in \{3, 5, 8, 10, 15\}$. As for the DTLZ test suite, the total number of decision variables is given by $n = m + k - 1$. k is set to 5 for DTLZ1, 10 for DTLZ2 to DTLZ4. For the WFG test instance, as suggested in [45], the number of decision variables is set as $n = k + l$, where $k = 2 * (m - 1)$ is the number of position-related variables and $l = 20$ is the number of distance-related variables.

4.2. MOEAs for Comparisons

In the experimental studies, we have selected four popular MOEAs for comparisons, namely, MOMBI-II [36], DBEA [37], MOEA/D-PBI [13], and RVEA [38]. MOMBI-II is an R2 indicator based MOEA; MOEA/D-PBI and DBEA are two decomposition based MOEAs; and as aforementioned, RVEA [38] is a state-of-the-art MOEA for solving MaOPs, where the reference vector guided selection strategy and the angle penalized distance metric are specifically tailored for many-objective optimization. In the following paragraphs, we present different parameter settings for each compared algorithm.

Table 2: Settings of the population size N, the boundary layer parameter $H1$ and the inside layer parameter $H2$.

Parameters	$m = 3$	$m = 5$	$m = 8$	$m = 10$	$m = 15$
($H1$,$H2$)	(12,0)	(6,0)	(3,2)	(3,2)	(2,1)
N	91	210	156	275	135

1) Population size: the settings of population size N for different numbers of objectives are summarized in Table 2. They are determined by the two design factors $H1$ and $H2$ together with the objective number m. $H1$ and $H2$ are used to generate uniformly distributed reference vectors on the outer boundaries and the inside layers, respectively. The size of reference vector set is equal to the population size.

2) SBX and PM operators: the reproduction procedure consists of the SBX [41] operator and the PM operator [42]. More specifically, as for the SBX operator, the distribution index is set to $\eta_c = 30$ in TS-R2EA, MOMBI-II, DBEA and RVEA while $\eta_c = 20$ in MOEA/D-PBI algorithm, and the crossover probability is $p_c = 1.0$ in all algorithms, as recommended in [36] and [38]. As for the PM operator, the distribution index is set to $\eta_m = 20$ and its mutation probability is $p_m = 1/n$, as recommended in [2].

3) Specific parameter settings in each algorithm: For MOMBI-II, the threshold of variance, the tolerance threshold and the *record* size of nadir vectors are set to 0.5, 0.001 and 5, respectively, as recommended in [36]. For DBEA, there is no additional parameter to be specified. For MOEA/D-PBI, the neighborhood size T is set to 20, and the penalty parameter θ in the penalty-based boundary intersection (PBI) approach is set as 5.0, as recommended in [13]. For RVEA and TS-R2EA, the index α used to control the rate of the convergence and diversity is set as $\alpha = 2.0$ and the reference vectors are adaptively updated using a parameter $f_r = 0.1$, as recommended in [38]. For all the MOEAs, *Gen* is the maximal number of generations, which are summarized in Table 3. The source code of MOMBI-II and DBEA is provided by the authors. MOEA/D-PBI and RVEA are implemented in the PlatEMO [46].

Table 3: The maximal number of generations *Gen* for different test instances.

Problems	$m = 3$	$m = 5$	$m = 8$	$m = 10$	$m = 15$
DTLZ1	400	600	750	1000	1500
DTLZ2	250	350	500	750	1000
DTLZ3	1000	1000	1000	1500	2000
DTLZ4	600	1000	1250	2000	3000
WFG1-WFG9	400	750	1500	2000	3000

4.3. Performance Indicators

To assess the performance of each algorithm, we consider the following two widely used performance indicators, namely, the modified inverted generational

distance (IGD^+) [24, 25] and hypervolume (HV) [21]. Both of them can simultaneously assess the convergence quality and diversity quality of a given solution set.

The IGD^+ is calculated with respect to a set of reference points sampled on the true Pareto front. In this work, the size of the reference set is the same as the number of reference vectors used in each algorithm. The HV is calculated with respect to a given reference point $z^r = (z_1^r, ..., z_m^r)^T$. $z^r = (1, 1, ..., 1)^T$ is used for DTLZ1 and $z^r = (2, 2, ..., 2)^T$ for DTLZ2, DTLZ3 and DTLZ4 test instances while $z^r = (3, 5, ..., 2m+1)^T$ is used for WFG1 to WFG9. For problems with fewer than 5 objectives, the recently proposed fast hypervolume calculation method is adopted to calculate the exact hypervolume, while for 5-, 8-, 10- and 15-objective problems, the Monte Carlo method with 1,000,000 sampling points is adopted to obtain the approximate hypervolume values. All the experiments have been independently run for 21 times. The statistical experimental results of IGD^+ and HV are summarized in the corresponding tables for performance comparison, where the Wilcoxon rank sum test at a significance level of 5% is further conducted to examine the statistical results obtained by TS-R2EA and the compared algorithms.

5. Experimental Results

In this section, the performance of TS-R2EA is assessed according to the experimental setup described in Section 4. Our experiments consist of five components. First of all, TS-R2EA is compared with MOMBI-II, DBEA, MOEA/D-PBI and RVEA on the DTLZ test problems. Secondly, we compare these algorithms on the WFG benchmark test problems. Thirdly, the effectiveness of the R2 indicator based primary selection and the reference vector guided secondary selection is investigated. Moreover, different variants of TS-R2EA are further assessed in order to validate the effectiveness of the two-stage selection strategy which is based on both the R2 indicator and the reference vector guided objective space partition method. Finally, the parameter sensitivity analysis is also

performed on a representative subset of the DTLZ and WFG test instances.

5.1. Performance Comparisons on DTLZ Test Suite

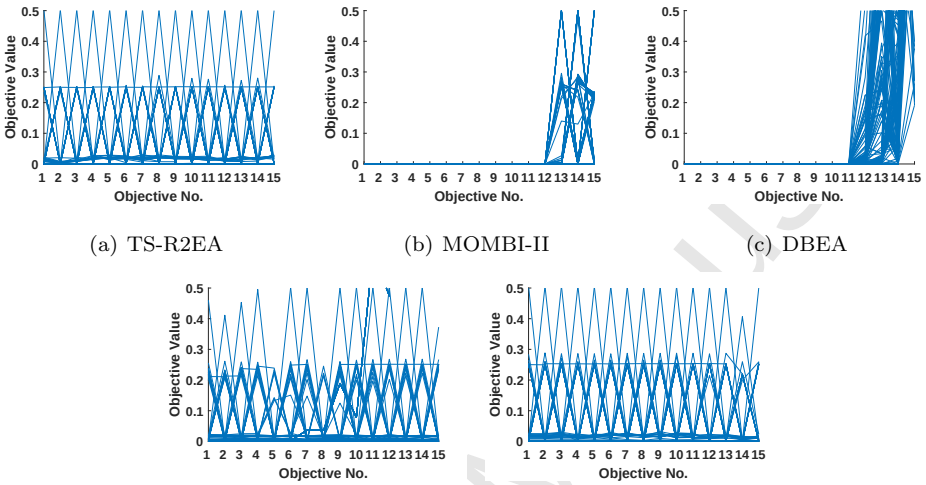

(a) TS-R2EA (b) MOMBI-II (c) DBEA

(d) MOEA/D-PBI (e) RVEA

Figure 4: The representation of the nondominated solutions obtained by each algorithm on the fifteen-objective DTLZ1 instance with the median IGD^+ value.

The main challenge of DTLZ1 lies in the large number of local PFs. As indicated by the statistical results via adopting Wilcoxon rank sum test in Tables 4 and 5, TS-R2EA has achieved the competitive performance among the other compared algorithms. MOMBI-II, DBEA and MOEA/D-PBI perform significantly worse than TS-R2EA as well as RVEA. As can be further observed from Fig. 4, the representation of the nondominated solutions obtained by each algorithm on DTLZ1 with 15-objective, which further confirms the outstanding performance of TS-R2EA in terms of both convergence and diversity of the obtained candidate solutions.

DTLZ2 is a relatively simple test problem with a spherical PF compared with DTLZ1. From the statistical results in Tables 4 and 5, TS-R2EA shows a competitive performance among the remaining algorithms especially in high-dimensional objective space in terms of both IGD^+ and HV values. By contrast,

Table 4: Statistical results (mean values and standard deviations) of IGD^+ values obtained by each algorithm on the DTLZ test suite. Best performance is shown in gray background. +, ≈ and − denote that TS-R2EA performs significantly better than, equivalent to, and worse than the compared algorithm, respectively.

IGD^+	m	TS-R2EA		MOMBI-II		DBEA		MOEA/D-PBI		RVEA	
DTLZ1	3	2.209E−03	+	2.455E−02	+	5.749E−03	+	4.162E−03	+	2.600E−03	
		1.068E−03		2.107E−03		4.213E−03		2.543E−03		1.368E−03	
	5	1.404E−03	+	6.928E−02	+	2.078E−01	+	4.152E−03	−	1.080E−03	
		5.054E−04		5.295E−03		3.068E−01		4.867E−03		2.847E−04	
	8	3.433E−03	+	1.570E−01	+	5.946E−01	+	2.448E−02	+	4.566E−03	
		4.971E−04		4.644E−03		4.566E−01		2.695E−02		2.104E−03	
	10	3.045E−03	+	1.741E−01	+	2.956E−01	+	4.040E−02	+	4.615E−03	
		4.982E−04		2.970E−03		6.897E−02		4.730E−02		2.420E−03	
	15	3.945E−03	+	2.551E−01	+	9.124E−01	+	2.278E−01	+	7.527E−03	
		2.159E−03		1.216E−02		5.383E−01		6.028E−01		4.630E−03	
DTLZ2	3	4.746E−03	+	3.355E−02	+	2.086E−02	−	3.704E−03	−	3.856E−03	
		6.340E−04		1.419E−03		4.485E−03		6.126E−04		6.714E−04	
	5	7.966E−03	+	1.025E−01	+	3.377E−02	−	3.263E−03	−	5.208E−03	
		7.271E−04		2.034E−04		9.886E−03		3.545E−04		5.291E−04	
	8	1.323E−02	+	3.937E−01	+	5.464E−02	+	1.852E−02	−	9.805E−03	
		1.259E−03		1.071E−02		8.751E−03		4.071E−02		8.796E−04	
	10	1.218E−02	+	4.959E−01	+	5.887E−02	−	7.867E−03	−	9.006E−03	
		9.831E−04		1.012E−02		9.357E−03		2.647E−03		6.251E−04	
	15	5.770E−03	+	7.533E−01	+	9.057E−01	+	2.336E−01	+	2.712E−02	
		8.919E−04		1.089E−02		3.354E−09		3.757E−01		7.072E−02	
DTLZ3	3	1.151E−02	+	3.517E−02	+	3.604E−01	+	1.669E−02	≈	1.078E−02	
		6.978E−03		2.290E−03		9.289E−01		5.591E−03		3.340E−03	
	5	9.872E−03	+	1.375E−01	+	1.894E−02	+	5.426E−01	≈	7.858E−03	
		3.933E−03		1.220E−02		1.433E−02		1.240E+00		3.192E−03	
	8	2.100E−02	+	4.239E−01	+	7.446E−01	+	1.087E+01	≈	2.094E−02	
		7.487E−03		4.948E−03		1.346E−01		2.932E+01		6.053E−03	
	10	1.272E−02	+	4.978E−01	+	8.339E−01	+	1.852E−02	−	1.052E−02	
		2.230E−03		5.888E−03		1.835E−05		7.665E−03		1.703E−03	
	15	1.051E−02	+	7.438E−01	+	9.058E−01	+	2.819E+01	+	2.313E−02	
		3.975E−03		4.329E−03		7.437E−05		4.665E+01		4.264E−02	
DTLZ4	3	2.382E−03	+	5.176E−02	+	1.043E−01	+	6.817E−02	−	1.872E−03	
		3.148E−04		6.169E−02		1.169E−01		1.214E−01		1.588E−03	
	5	4.030E−03	+	1.024E−01	+	1.455E−01	+	3.396E−02	−	1.759E−03	
		3.595E−04		2.506E−04		1.024E−01		5.648E−02		1.203E−04	
	8	1.106E−02	+	3.983E−01	+	1.441E−01	+	7.037E−02	+	1.701E−02	
		1.640E−02		1.873E−02		3.979E−02		5.196E−02		2.854E−02	
	10	6.684E−03	+	5.095E−01	+	1.157E−01	+	5.907E−01	+	1.241E−02	
		4.701E−04		3.162E−02		1.903E−02		9.779E−02		1.893E−02	
	15	1.852E−02	+	7.684E−01	+	9.058E−01	+	1.115E−01	+	2.271E−02	
		2.128E−02		3.541E−02		8.203E−05		1.804E−01		2.886E−02	
+/ ≈ /−				20/0/0		20/0/0		17/0/3		9/3/8	

Table 5: Statistical results (mean values and standard deviations) of HV values obtained by each algorithm on the DTLZ test suite. Best performance is shown in gray background. +, ≈ and − denote that TS-R2EA performs significantly better than, equivalent to, and worse than the compared algorithm, respectively.

HV	m	TS-R2EA		MOMBI-II		DBEA		MOEA/D-PBI		RVEA
DTLZ1	3	9.732E−01 2.430E−04	+	9.662E−01 1.971E−04	+	9.725E−01 9.809E−04	+	9.726E−01 9.033E−04	+	9.731E−01 3.087E−04
	5	9.990E−01 7.870E−05	+	9.966E−01 7.138E−04	+	8.266E−01 3.114E−01	+	9.979E−01 2.220E−04	+	9.984E−01 4.051E−05
	8	9.995E−01 1.281E−05	+	9.879E−01 1.665E−03	+	5.691E−01 3.179E−01	+	9.940E−01 1.583E−02	≈	9.991E−01 4.807E−06
	10	9.995E−01 2.236E−07	+	9.901E−01 7.871E−04	+	8.617E−01 1.082E−01	+	9.629E−01 8.963E−02	+	9.980E−01 9.119E−07
	15	9.995E−01 1.325E−06	+	9.494E−01 4.157E−03	+	3.438E−01 3.394E−01	+	7.913E−01 2.917E−01	+	9.947E−01 1.270E−05
DTLZ2	3	7.406E+00 1.202E−03	+	7.376E+00 2.402E−03	+	7.398E+00 2.601E−03	≈	7.406E+00 3.132E−03	−	7.407E+00 1.041E−03
	5	3.167E+01 9.913E−03	+	3.154E+01 1.407E−02	+	3.166E+01 1.096E−02	−	3.169E+01 9.302E−03	−	3.168E+01 2.530E−03
	8	2.558E+02 2.057E−02	+	2.456E+02 6.822E−01	+	2.556E+02 2.426E−02	+	2.556E+02 3.238E−01	−	2.559E+02 7.823E−03
	10	1.024E+03 2.166E−02	+	9.789E+02 3.026E+00	≈	1.022E+03 2.945E−02	≈	1.023E+03 2.876E−02	+	1.021E+03 8.784E−03
	15	3.277E+04 7.300E−02	+	2.921E+04 2.144E+02	+	1.638E+04 5.359E−05	+	3.007E+04 5.887E+03	≈	3.276E+04 7.317E−02
DTLZ3	3	7.393E+00 1.280E−02	+	7.376E+00 7.492E−03	+	5.639E+00 6.946E+00	+	4.243E+00 5.432E−03	−	7.399E+00 6.011E−03
	5	3.166E+01 1.319E−02	+	3.132E+01 8.397E−02	+	3.165E+01 2.206E−02	+	2.704E+01 8.866E+00	≈	3.169E+01 7.199E−03
	8	2.556E+02 1.707E−02	+	2.434E+02 6.455E−01	+	1.446E+02 3.553E+01	+	2.174E+02 9.369E+01	−	2.558E+02 9.928E−03
	10	1.024E+03 3.262E−02	+	9.780E+02 3.660E+00	+	5.120E+02 9.396E−03	≈	1.023E+03 2.990E−02	+	1.022E+03 1.034E−02
	15	3.277E+04 1.200E−01	+	2.906E+04 3.278E+02	+	1.638E+04 1.218E+00	+	1.472E+04 1.670E+04	≈	3.276E+04 1.410E−01
DTLZ4	3	7.410E+00 5.599E−04	+	7.282E+00 3.007E−01	+	6.995E+00 5.262E−01	+	7.023E+00 8.105E−01	≈	7.411E+00 2.812E−03
	5	3.169E+01 7.533E−03	+	3.154E+01 1.147E−02	+	3.100E+01 7.058E−01	+	3.156E+01 2.391E−01	−	3.170E+01 3.212E−03
	8	2.558E+02 6.298E−02	+	2.456E+02 5.537E−01	+	2.554E+02 3.248E−01	+	2.556E+02 2.754E−01	+	2.557E+02 8.127E−02
	10	1.024E+03 2.769E−02	+	9.784E+02 2.968E+00	+	1.020E+03 8.992E−02	+	8.596E+02 1.476E+02	+	1.022E+03 3.100E−02
	15	3.277E+04 1.456E−01	+	2.931E+04 2.459E+02	+	1.638E+04 1.344E+00	+	3.250E+04 8.466E+02	+	3.276E+04 1.347E−01
+/ ≈ /−				20/0/0		19/1/0		16/3/1		9/5/6

MOEA/D-PBI and RVEA have obtained the better convergence and diversity on the instances with 3-, 5- and 8-objective. MOMBI-II and DBEA are slightly outperformed by TS-R2EA.

DTLZ3 is a highly multimodal problem in order to verify whether an MOEA has the ability to jump out of local PFs. The performance of TS-R2EA and RVEA is significantly better than the other three compared algorithms on all instances with 3 to 15 objectives as shown in Tables 4 and 5. To be specific, RVEA is more suitable for coping with instances with 3-, 5- and 10-objective, whereas TS-R2EA has achieved the better performance on the 15-objective instance.

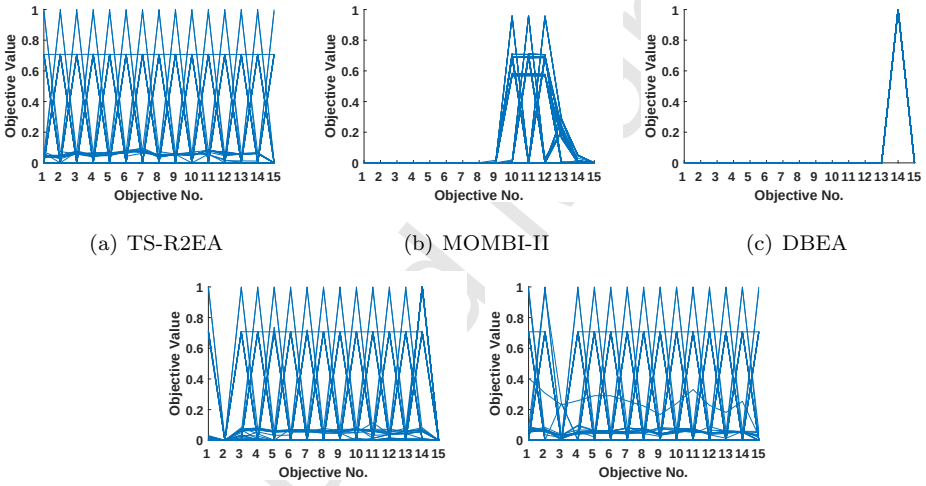

(a) TS-R2EA (b) MOMBI-II (c) DBEA

(d) MOEA/D-PBI (e) RVEA

Figure 5: The representation of the nondominated solutions obtained by each algorithm on the fifteen-objective DTLZ4 instance with the median IGD^+ value.

DTLZ4 is designed to investigate an algorithm's ability to maintain the distribution of candidate solutions given that the PF is highly biased. According to the Tables 4 and 5, TS-R2EA shows better performance on instances with 8-, 10- and 15-objective in terms of both IGD^+ and HV values. By contrast, RVEA is more suitable for dealing with instances with 3- and 5-objective; MOMBI-II, DBEA and MOEA/D-PBI perform significantly worse than TS-R2EA and RVEA. Fig. 5 gives the parallel coordinates of the nondominated solutions ob-

tained by each algorithm on 15-objective DTLZ4 with the median IGD^+ value. TS-R2EA is able to achieve a well converged and widely distributed approximation PF. MOMBI-II, DBEA and MOEA/D-PBI are only able to obtain some parts of the true PF due to the biased distribution of the candidate solutions. Fig. 5 (e) shows that RVEA performs better than the traditional R2 indicator and decomposition based evolutionary algorithms. Nevertheless, the overall best optimizer is still the proposed TS-R2EA, especially in high-dimensional objective space as shown in Fig. 5 (a). This is due to the fact that the two-stage selection strategy in TS-R2EA is able to well balance convergence and diversity, which is particularly meaningful in high-dimensional objective spaces.

In order to validate the experimental results, the supplementary material gives the statistical results by the two-sided sign test at a significance level of 5% [47]. Similar to the observations obtained by adopting the Wilcoxon rank sum test, TS-R2EA and RVEA also perform best on most of 20 comparisons and significantly outperform other compared algorithms on DTLZ1-DTLZ4.

5.2. Performance Comparisons on WFG Test Suite

WFG1 is introduced to test the ability of each algorithm to tackle flat bias and mixed structure of the PF. As shown in Table 6, despite that TS-R2EA is slightly outperformed by MOMBI-II in terms of HV values, its performance is significantly better than the remaining MOEAs. WFG2 tests the optimizer's ability to deal with disconnected PF. MOMBI-II has obtained the best HV values on instances with 3 to 10 objectives, and DBEA and MOEA/D-PBI show poor performance on this problem. By contrast, the proposed TS-R2EA is the second-best algorithm on it. The PF shape of WFG3 which can be seen as the connected version of WFG2 is linear and degenerate. In term of HV values in Table 6, the overall performance of TS-R2EA is better than RVEA and DBEA, while MOMBI-II has obtained the best HV values among the compared algorithms in most cases.

The remaining six test problems have the same PF shape in the objective space while their characteristics are different in the decision variable space. More

Table 6: Comparisons of median HV values obtained by each algorithm on the WFG test suite. Best performance is shown in gray background. +, ≈ and − denote that TS-R2EA performs significantly better than, equivalent to, and worse than the compared algorithm, respectively.

HV	m	TS-R2EA		MOMBI-II		DBEA		MOEA/D-PBI		RVEA	
WFG1	3	5.021E+01	+	4.970E+01	+	4.843E+01	+	8.062E+00	+	4.812E+01	
	5	4.674E+03	−	7.495E+03	+	4.289E+03	+	1.020E+03	+	4.347E+03	
	8	1.535E+07	−	3.269E+07	−	1.994E+07	+	3.645E+06	+	1.233E+07	
	10	6.199E+09	−	1.339E+10	≈	9.675E+09	+	1.603E+09	+	4.874E+09	
	15	9.620E+16	−	1.777E+17	≈	6.224E+16	+	2.263E+16	≈	8.928E+16	
WFG2	3	9.246E+01	≈	9.584E+01	+	9.000E+01	+	8.486E+01	+	9.032E+01	
	5	9.683E+03	−	1.026E+04	≈	9.712E+03	+	9.357E+03	≈	9.891E+03	
	8	3.031E+07	−	3.314E+07	≈	2.422E+07	+	2.828E+07	≈	2.971E+07	
	10	1.268E+10	−	1.338E+10	+	9.010E+09	+	1.178E+10	≈	1.250E+10	
	15	1.606E+17	≈	1.614E+17	+	7.950E+16	≈	1.449E+17	≈	1.657E+17	
WFG3	3	7.334E+01	−	7.455E+01	+	7.019E+01	+	6.315E+01	+	6.896E+01	
	5	6.870E+03	+	6.678E+03	+	6.566E+03	+	5.972E+03	+	6.150E+03	
	8	1.521E+07	−	2.285E+07	+	2.017E+06	≈	1.500E+07	+	1.023E+07	
	10	4.426E+09	−	9.230E+09	+	6.523E+08	−	5.514E+09	+	3.574E+09	
	15	3.839E+16	−	1.178E+17	+	6.122E+15	−	4.973E+16	≈	3.964E+16	
WFG4	3	7.181E+01	−	7.295E+01	+	7.082E+01	+	6.815E+01	−	7.296E+01	
	5	8.555E+03	+	7.992E+03	+	8.442E+03	+	8.347E+03	≈	8.581E+03	
	8	3.009E+07	+	1.931E+07	≈	3.024E+07	+	1.766E+07	+	2.939E+07	
	10	1.263E+10	+	8.003E+09	−	1.300E+10	+	4.389E+09	+	1.224E+10	
	15	1.800E+17	+	7.077E+16	+	7.814E+16	+	5.525E+16	+	1.092E+17	
WFG5	3	7.043E+01	+	6.991E+01	+	6.953E+01	+	6.548E+01	−	7.091E+01	
	5	8.475E+03	+	7.357E+03	+	8.442E+03	+	8.007E+03	−	8.491E+03	
	8	3.041E+07	+	1.769E+07	+	2.966E+07	+	1.479E+07	≈	3.032E+07	
	10	1.256E+10	+	6.757E+09	+	1.233E+10	+	3.467E+09	+	1.248E+10	
	15	1.773E+17	+	6.086E+16	+	3.983E+16	+	3.379E+16	+	1.764E+17	
WFG6	3	7.048E+01	≈	7.092E+01	+	6.969E+01	+	6.610E+01	≈	7.099E+01	
	5	8.581E+03	+	6.981E+03	≈	8.576E+03	+	7.638E+03	≈	8.612E+03	
	8	3.045E+07	+	1.698E+07	≈	3.063E+07	+	1.327E+07	+	3.014E+07	
	10	1.262E+10	+	6.985E+09	≈	1.261E+10	+	3.269E+09	≈	1.254E+10	
	15	1.781E+17	+	5.969E+16	+	7.101E+16	+	3.283E+16	≈	1.730E+17	
WFG7	3	7.207E+01	−	7.239E+01	≈	7.096E+01	+	1.626E+01	≈	6.214E+01	
	5	8.586E+03	+	7.657E+03	−	8.989E+03	+	1.937E+03	+	5.232E+03	
	8	2.052E+07	≈	1.698E+07	≈	1.727E+07	+	3.739E+06	+	1.049E+07	
	10	8.178E+09	≈	7.921E+09	≈	7.167E+09	+	1.386E+09	+	4.646E+09	
	15	6.247E+16	≈	6.647E+16	+	5.211E+16	+	1.758E+16	+	2.225E+16	
WFG8	3	4.305E+01	−	4.837E+01	+	4.025E+01	+	3.313E+01	+	4.104E+01	
	5	5.065E+03	+	4.009E+03	+	4.927E+03	+	3.486E+03	+	4.427E+03	
	8	9.534E+06	−	1.380E+07	−	1.449E+07	+	5.756E+06	+	7.060E+06	
	10	3.901E+09	−	5.844E+09	+	1.377E+09	+	1.903E+09	+	3.239E+09	
	15	4.404E+16	−	5.055E+16	+	6.720E+15	+	7.069E+15	+	2.118E+16	
WFG9	3	6.748E+01	+	6.582E+01	+	6.736E+01	+	6.245E+01	≈	6.745E+01	
	5	7.818E+03	+	6.439E+03	+	7.805E+03	+	7.431E+03	+	7.184E+03	
	8	2.493E+07	+	1.651E+07	−	2.623E+07	+	2.069E+07	+	1.958E+07	
	10	1.044E+10	+	6.551E+09	≈	1.021E+10	+	9.072E+09	+	6.624E+09	
	15	1.054E+17	+	5.774E+16	+	4.797E+15	≈	1.083E+17	+	5.752E+16	
+/ ≈ /−				22/6/17		28/12/5		40/3/2		28/14/3	

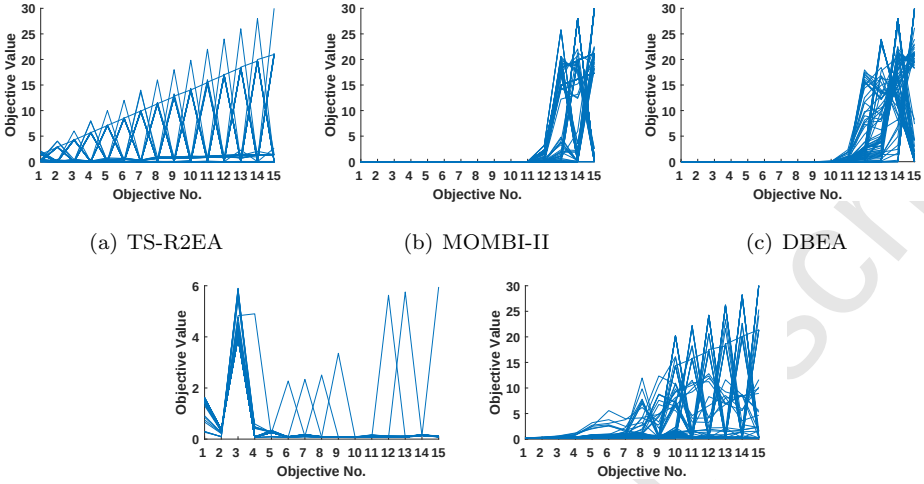

(a) TS-R2EA (b) MOMBI-II (c) DBEA

(d) MOEA/D-PBI (e) RVEA

Figure 6: The representation of the nondominated solutions obtained by five algorithms on the fifteen-objective WFG4 instance with the median HV value.

specifically, WFG4 is a multi-frontal optimization problem with a concave PF. As shown by the statistical results in Table 6, RVEA has obtained the best performance on instances with 3- and 5-objective, while DBEA has achieved the best performance on instances with 8- and 10-objective. TS-R2EA achieves the competitive performance when the number of objectives is 15. As further observed in Fig. 6, TS-R2EA can obtain well converged and widely spreading solution sets close to the true Pareto fronts on 15-objective WFG4 test instance.

Regarding WFG5, which introduces deceptive characteristic in decision variable space, TS-R2EA shows a competitive performance compared with the other algorithms, especially in high-dimensional objective space while RVEA has obtained best performance on instances with 3- and 5-objective as shown in Table 6.

For WFG6, which is designed with nonseparable and reduced characteristics, TS-R2EA still achieves the competitive performance on 10- and 15-objective instances, whereas RVEA has achieved the better performance on instances with 3- and 5-objective as illustrated in Table 6. DBEA has a competitive

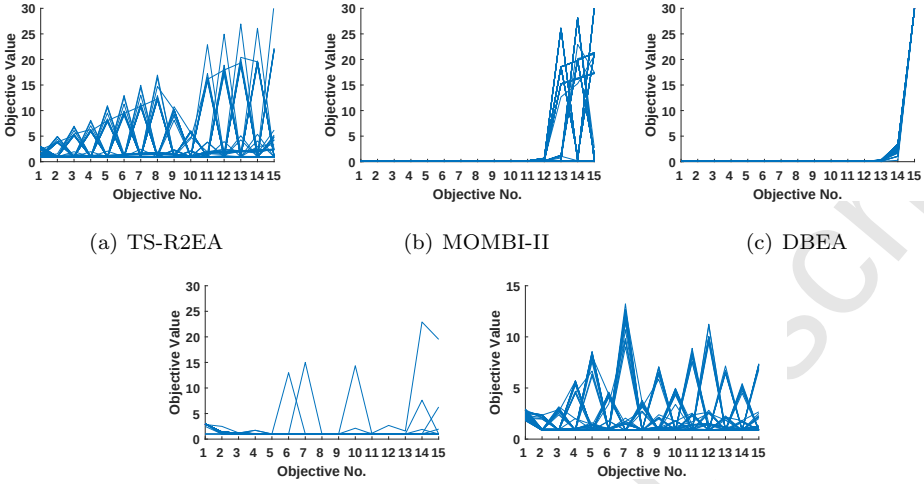

(a) TS-R2EA (b) MOMBI-II (c) DBEA

(d) MOEA/D-PBI (e) RVEA

Figure 7: The representation of the nondominated solutions obtained by five algorithms on the fifteen-objective WFG8 instance with the median HV value.

performance with respect to TS-R2EA on instances with 5-, 8- and 10-objective in term of HV values. MOMBI-II and MOEA/D-PBI perform worst on most instances of WFG6, where it obtains the smallest HV values.

WFG7 is a separable and uni-modal problem with parameter dependency. In terms of HV values, TS-R2EA, MOMBI-II and DBEA have obtained similar performance. RVEA and MOEA/D-PBI are not quite suitable for solving WFG7.

Concerning the WFG8 test instance, which has a higher parameter dependency, MOMBI-II is the best optimizer as evidenced by Table 6 and Fig. 7. To be specific, MOMBI-II is able to converge to the true PF while TS-R2EA achieves the better distribution as illustrated in Fig. 7 (b) and (a), respectively. In addition, TS-R2EA shows the better performance when the number of objective is 5, and DBEA has obtained the best performance for 8-objective instance.

WFG9 is a difficult problem due to the characteristics of non-separability, multi-modality, deceptiveness and parameter bias. As a result, TS-R2EA has

shown the most competitive overall performance while DBEA and MOEA/D-PBI have obtained promising results for 8- and 15-objective instances, respectively. By contrast, the performance of MOMBI-II and RVEA are significantly worse than TS-R2EA.

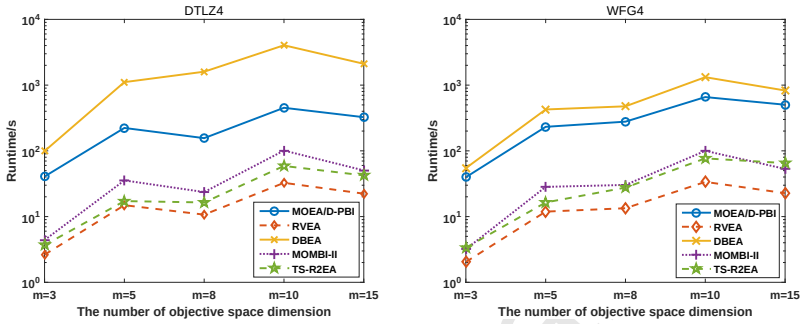

(a) The runtime of DTLZ4 (b) The runtime of WFG4

Figure 8: The computational time required by TS-R2EA, MOMBI-II, DBEA, MOEA/D-PBI and RVEA for the DTLZ4 and WFG4 test instances, respectively.

As shown by the results in Table 6, Fig. 6, Fig. 7, in summary, none of the five algorithms is able to perform very well on all of the nine test problems. To be specific, TS-R2EA can properly deal with WFG4, WFG5, WFG6, WFG7 and WFG9 while MOMBI-II has achieved the best HV values on WFG1, WFG2, WFG3 and WFG8; DBEA is suitable for solving medium-scale problems, especially on WFG4, WFG6, WFG7 and WFG8; RVEA has achieved the best performance on 3- and 5-objective WFG4, WFG5 and WFG6 test instances. After considering the supplementary material, the statistical results show the similar observation by adopting the Wilcoxon rank sum test. Fig. 8 shows the average computational time required by each of the compared algorithms on the DTLZ4 and WFG4 test instances with 3 to 15 objectives. We can observe that the proposed algorithm performs the medium computational efficiency between RVEA and MOMBI-II. The other two compared algorithms, DBEA and MOEA/D-PBI, take substantially more computational time. In summary, it can be concluded that RVEA is the most efficient among the compared algorithms

while the computational complexity of TS-R2EA is also acceptable.

5.3. Assessment of Primary and Secondary Selections in TS-R2EA

The TS-R2EA selection strategy consists of two selection stages: the R2 indicator based primary selection and the reference vector guided secondary selection. Therefore, P_{R2} and P_{RV} will be preserved after employing the two-stage selection mechanism. Furthermore, to assess the effectiveness of the two selection stages, the proportion of the candidate solutions selected via each of them is recorded. Specifically, the proportion of the candidate solutions selected by the primary strategy is defined as $P_{R2}/(P_{R2}+P_{RV})$ while $P_{RV}/(P_{R2}+P_{RV})$ is the proportion of the candidate solutions selected by the secondary selection method.

For the DTLZ test suite, the two-stage selection strategy plays a crucial role in balancing convergence and diversity especially for 15-objective problems. For example, DTLZ1 is a challenging problem for most MOEAs due to a large number of local fronts in the objective space. As shown in Fig. 9 (a), the reference vector guided secondary selection is essential for maintaining a proper population diversity to escape from local optima at the early search stage; meanwhile, the R2 indicator based selection plays a dominant role in the later search stage. Another example is the 15-objective DTLZ4 which has a strongly biased Pareto set. As shown in Fig. 9 (b), the candidate solutions selected via the R2 indicator always occupies the majority of the offspring population, especially as the number of generation increases. Generally, the secondary selection strategy can comprehensively balance the convergence and diversity by interacting with the primary selection at an earlier stage of the evolutionary procedure. In addition, since the Pareto fronts of DTLZ1 to DTLZ4 are of regular shapes, which are consistent with the distribution of the predefined reference vectors, the proportion of the candidate solutions selected by the secondary selection strategy is almost zero at the later stage of the evolutionary procedure as shown in Fig. 9 (a) and (b).

For the WFG test suite, the two-stage selection strategy also plays an im-

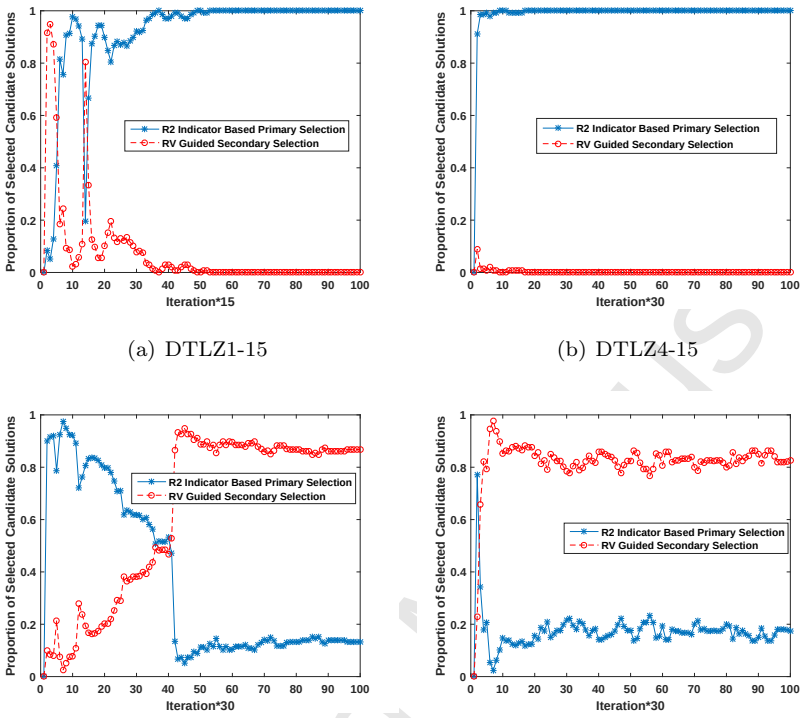

(a) DTLZ1-15 (b) DTLZ4-15

(c) WFG4-15 (d) WFG6-15

Figure 9: The proportion of candidate solutions selected via the R2 based primary selection and the reference vector (RV) guided secondary selection on some typical DTLZ and WFG problems.

portant role, though the observations are a little different from those obtained on the DTLZ test suite. To clarify the two-stage selection strategy, we take WFG4 and WFG6 with 15 objectives as examples. As shown in Fig. 9 (c) and (d), the proportion of the candidate solutions selected by the primary selection is dominant at the early stage while the importance of the reference vector guided secondary selection increases rapidly as the number of iterations increases. More specifically, the primary selection plays a dominant role at the early evolutionary stage in Fig. 9 (c), and as the number of iterations increases, the secondary selection begins to play a dominant role. The final proportion of the candidate solutions selected by the primary and secondary selections are

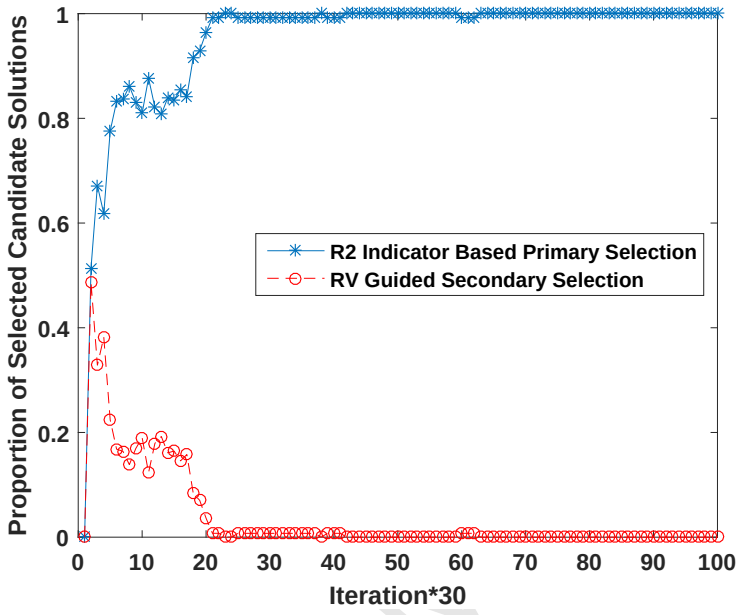

Figure 10: The proportion of candidate solutions selected via the R2 based primary selection and the reference vector (RV) guided secondary selection (without reference vector adaptation) on the 15-objective WFG4.

about 85% and 15% respectively.

In Fig. 9, it is interesting to see that the proposed two-stage selection strategy performs slightly different when solving the DTLZ and WFG problems. This is due to the fact that the objectives of the WFG problems are scaled to different ranges, which will frequently trigger the adaptation of candidate solutions selected by the reference vector guided secondary selection. By contrast, since the objectives of the DTLZ problems are normalized, the distribution of the candidate solutions is relatively more stable. In order to examine this observation, we conduct an additional experiment by disabling the reference vector adaptation strategy in the secondary selection in TS-R2EA. Consequently, as shown in Fig. 10, TS-R2EA shows stable performance as those in 9 (a) and (b).

Table 7: HV values obtained by different variants of TS-R2EA on DTLZ and WFG benchmark test problems. Best performance is shown in gray background. $+$, $\approx$ and $-$ denote that TS-R2EA performs significantly better than, equivalent to, and worse than the other three variants, respectively.

HV	m	TS-R2EA		TS-R2EA-$v1$		TS-R2EA-$v2$		TS-R2EA-$v3$
DTLZ1	10	9.995E-01	$+$	9.993E-01	$\approx$	9.994E-01	$+$	9.992E-01
	15	9.995E-01	$\approx$	9.993E-01	$\approx$	9.994E-01	$+$	9.992E-01
DTLZ2	10	1.024E+03	$\approx$	1.023E+03	$+$	1.022E+03	$+$	1.021E+03
	15	3.277E+04	$+$	3.271E+04	$\approx$	3.276E+04	$\approx$	3.275E+04
DTLZ3	10	1.024E+03	$\approx$	1.023E+03	$\approx$	1.022E+03	$\approx$	1.023E+03
	15	3.276E+04	$\approx$	3.276E+04	$\approx$	3.275E+04	$\approx$	3.277E+04
DTLZ4	10	1.024E+03	$\approx$	1.023E+03	$\approx$	1.023E+03	$\approx$	1.021E+03
	15	3.276E+04	$-$	3.277E+04	$-$	3.277E+04	$\approx$	3.277E+04
WFG1	10	6.199E+09	$-$	6.672E+09	$+$	5.026E+09	$-$	9.156E+09
	15	9.620E+16	$\approx$	1.017E+17	$+$	8.210E+16	$+$	7.282E+16
WFG2	10	1.268E+10	$+$	1.180E+10	$+$	1.184E+10	$+$	1.158E+10
	15	1.606E+17	$\approx$	1.652E+17	$+$	1.570E+17	$+$	1.477E+17
WFG3	10	4.426E+09	$-$	5.090E+09	$-$	6.525E+09	$+$	3.928E+09
	15	3.839E+16	$+$	3.503E+16	$\approx$	4.944E+16	$+$	3.473E+16
WFG4	10	1.263E+10	$+$	1.143E+10	$+$	1.224E+10	$+$	1.082E+10
	15	1.800E+17	$+$	1.574E+17	$+$	1.249E+17	$+$	1.269E+17
WFG5	10	1.256E+10	$+$	1.149E+10	$+$	1.194E+10	$+$	1.105E+10
	15	1.773E+17	$+$	1.587E+17	$+$	1.575E+17	$+$	9.745E+16
WFG6	10	1.262E+10	$+$	1.164E+10	$+$	1.210E+10	$+$	1.061E+10
	15	1.781E+17	$+$	1.352E+17	$+$	1.499E+17	$+$	7.766E+16
WFG7	10	8.178E+09	$\approx$	7.979E+09	$+$	4.729E+09	$\approx$	8.073E+09
	15	6.247E+16	$\approx$	5.719E+16	$+$	3.323E+16	$\approx$	6.066E+16
WFG8	10	3.901E+09	$+$	3.101E+09	$+$	3.549E+09	$+$	2.589E+09
	15	4.404E+16	$+$	2.102E+16	$+$	3.197E+16	$+$	7.459E+15
WFG9	10	1.044E+10	$+$	9.300E+09	$+$	8.299E+09	$+$	9.060E+09
	15	1.054E+17	$\approx$	1.015E+17	$+$	6.523E+16	$\approx$	1.003E+17
$+/\approx/-$				13/10/3		17/7/2		17/8/1

5.4. Different Variants of TS-R2EA

The aforementioned experimental results as given in Section 5.1 and 5.2 have validated the competitive performance of TS-R2EA through comparative analyses. In the following, we further assess the effectiveness of the three main components in the proposed T2-R2EA, namely, the R2 indicator based selection strategy, the reference vector guided selection method and adaptive angle-penalized distance. To be specific, we conduct some experiments to compare three different variants of T2-R2EA:

1. *TS-R2EA-v1*: This variant adopts constant parameter 1 instead of adaptive penalty parameter in the APD utility function.
2. *TS-R2EA-v2*: In order to further assess the effectiveness of the APD metric, we first remove the primary R2 indicator based selection. Then, the PBI approach with $\theta = 5.0$, as recommended in [13], is adopted instead of the APD metric as the evaluation indicator in the secondary selection.
3. *TS-R2EA-v3*: In this variant, only the R2 indicator based primary selection is adopted, while the reference vector guided secondary selection is removed. The major purpose of this variant is to assess the effectiveness of reference vector guided objective space partition selection strategy.

As demonstrated by the experimental results in Table 7, compared with the three variants, TS-R2EA shows similar performance on the 10- and 15-objective DTLZ test instances, and significantly better performance on the high-dimensional WFG test instances. To be specific, as for TS-R2EA-$v1$ which adopts the constant parameter rather than the adaptive APD utility function, it shows poor performance on WFG4 to WFG9; as for TS-R2EA-$v2$ which only adopts reference vector guided selection strategy based on the PBI decomposition method, it fails to achieve a good balance between convergence and diversity for most of test instances. In addition, the effectiveness of the reference vector guided secondary selection strategy is also verified, as TS-R2EA performs better than, worse than and similar to TS-R2EA-$v3$ on 17, 1 and 8 out of 26 comparisons. Therefore, in summary, both stages in the selection strategy play

an essential and effective role for the proposed TS-R2EA to achieve a balanced convergence and diversity for high-dimensional many-objective optimization.

5.5. Parameter Sensitivity Analysis

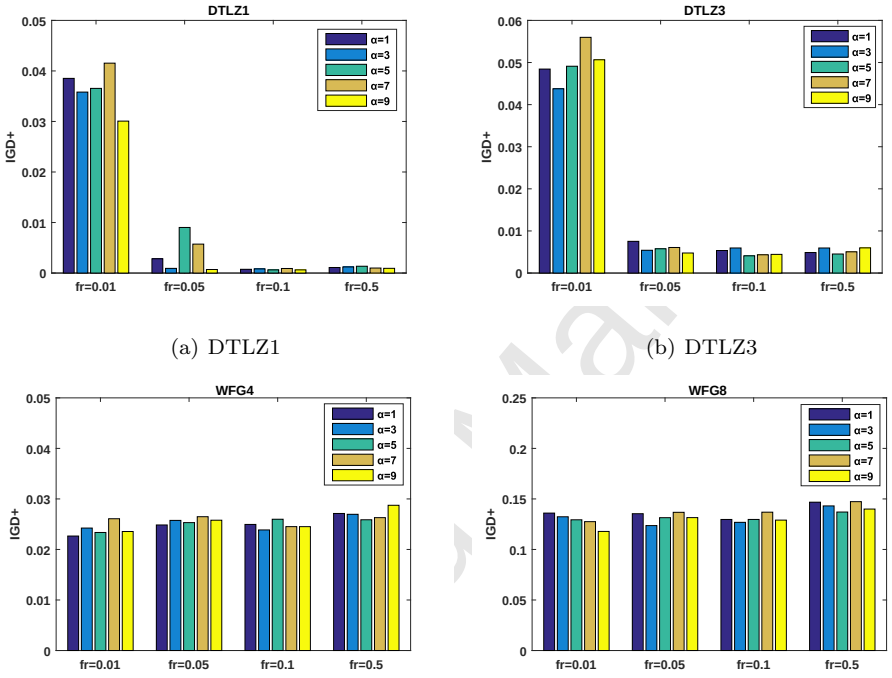

(a) DTLZ1 (b) DTLZ3

(c) WFG4 (d) WFG8

Figure 11: Median IGD$^+$ values obtained by TS-R2EA with 20 different combinations of f_r and α on DTLZ1, DTLZ3, WFG4 and WFG8 problems with three objectives.

There are two additional parameters to be specified in TS-R2EA: α which regulates the rates of changes of APD utility function and f_r which controls the frequency of employing the reference vector adaptation. To further study the sensitivity of the performance of TS-R2EA to the settings of f_r and α, we choose some special values for each parameter: $f_r \in \{0.01, 0.05, 0.1, 0.5\}$ and $\alpha \in \{1, 3, 5, 7, 9\}$, as recommended in [38]. The additional experiments are conducted on 3-objective test instances of DTLZ1, DTLZ3, WFG4 and WFG8, respectively, to compare the performance of all 20 different configurations. Each

configuration on each test instance has been run 21 times.

We first perform the sensitivity analysis of parameter f_r. In the light of Fig. 11 (a) and (b), the frequently used reference vector adaptation strategy, such as given by $f_r = 0.01$ or $f_r = 0.05$, will lead to a slight deterioration of TS-R2EA in terms of IGD$^+$ values on the DTLZ1 and DTLZ3 test instances. As shown in Fig. 11 (c) and (d), different combinations can lead to different characteristics on distinct test instances. To be specific, $f_r = 0.01$ is suitable for the WFG4 instance while the proper f_r for solving the WFG8 problem is 0.1. In addition, $f_r = 0.5$ is unsuitable for the WFG4 and WFG8 test instances. Based on these observations, we suggest that a medium value of f_r should be adopted (e.g. $f_r = 0.1$). Secondly, it turns out that different α shows the different performance in Fig. 11. Furthermore, it can be seen that $\alpha = 5$ and $\alpha = 7$ are not suitable for the DTLZ1 instance as illustrated in Fig. 11 (a). In addition, as indicated by Fig. 11 (c), the relatively larger α, such as $\alpha = 7$ and $\alpha = 9$, obtain the higher IGD$^+$ values. $\alpha = 1$ and $\alpha = 3$ show the similar performance on the respective DTLZ and WFG test suites. In general, it is better to choose $f_r = 0.1$, and α between 1 and 3.

6. Conclusion

This paper has proposed an enhanced R2 indicator based evolutionary algorithm, namely, TS-R2EA, for many-objective optimization. The algorithm adopts a two-stage selection strategy which combines the R2 indicator based primary selection and the reference vector guided secondary selection, where the motivation is to take advantages of both selection stages. In the proposed TS-R2EA, inspired by [38], a reference vector adaptation strategy has been adopted to deal with badly-scaled problems; and the convergence and diversity are well balanced by the angle penalized distance (APD) utility function.

According to the empirical results, TS-R2EA has shown highly competitive performance on benchmark problems up to fifteen objectives in comparison with four state-of-the-art MOEAs, namely, MOMBI-II, DBEA, MOEA/D-PBI and

RVEA. Besides, in order to analyze the effectiveness of the R2 based primary selection, the reference vector guided secondary selection and the adaptation mechanism, we have conducted some experiments to compare the performance of original TS-R2EA with three different variants as well. Our experimental results indicate that, by adopting the proposed two-stage selection together with the reference vector adaption strategy and the angle penalized distance (APD) utility function, TS-R2EA has achieved promising performance on many-objective optimization problems (MaOPs) with up to 15 objectives.

In the future, we would like to further investigate how to modify the proposed TS-R2EA algorithm to cope with constrained [48], or large-scale many-objective optimization problems [49].

Acknowledgment

This work was partially supported by the National Natural Science Foundation of China, under Grants 61773106,61374137, and the State Key Laboratory of Integrated Automation of Process Industry Technology and Research Center of National Metallurgical Automation Fundamental Research Funds, under Grant 2013ZCX02-03. The authors would like to thank the editors and anonymous reviewers for their valuable comments. Thanks to Prof. Carlos A. Coello Coello and his students for providing their source code.

References

[1] C. A. C. Coello, Evolutionary multi-objective optimization: a historical view of the field, Computational Intelligence Magazine, IEEE 1 (1) (2006) 28–36.

[2] K. Deb, Multi-objective optimization using evolutionary algorithms, Vol. 16, John Wiley & Sons, 2001.

[3] A. Zhou, B.-Y. Qu, H. Li, S.-Z. Zhao, P. N. Suganthan, Q. Zhang, Multiobjective evolutionary algorithms: a survey of the state of the art, Swarm and Evolutionary Computation 1 (1) (2011) 32 – 49.

[4] B. Li, J. Li, K. Tang, X. Yao, Many-objective evolutionary algorithms: a survey, ACM Comput. Surv. 48 (1) (2015) 1–35.

[5] H. Ishibuchi, N. Tsukamoto, Y. Nojima, Evolutionary many-objective optimization: a short review, in: Proceedings of the IEEE Congress on Evolutionary Computation, 2008, pp. 2419–2426.

[6] M. Farina, P. Amato, A fuzzy definition of "optimality" for many-criteria optimization problems, IEEE Transactions on Systems, Man, and Cybernetics - Part A: Systems and Humans 34 (3) (2004) 315–326.

[7] M. Köppen, R. Vicente-Garcia, B. Nickolay, Fuzzy-Pareto-dominance and its application in evolutionary multi-objective optimization, in: Proceedings of the Evolutionary Multi-criterion Optimization, Springer, 2005, pp. 399–412.

[8] S. Yang, M. Li, X. Liu, J. Zheng, A grid-based evolutionary algorithm for many-objective optimization, IEEE Transactions on Evolutionary Computation. 17 (5) (2013) 721–736.

[9] R. Wang, R. C. Purshouse, P. J. Fleming, Preference-inspired coevolutionary algorithm for many-objective optimization, IEEE Transactions on Evolutionary Computation. 17 (4) (2013) 474–494.

[10] M. Li, S. Yang, X. Liu, Shift-based density estimation for Pareto-based algorithm in many-objective optimization, IEEE Transactions on Evolutionary Computation. 18 (3) (2014) 348–365.

[11] X. Zhang, Y. Tian, Y. Jin, A knee point-driven evolutionary algorithm for many-objective optimization, IEEE Transactions on Evolutionary Computation. 19 (6) (2015) 761–776.

[12] T. Murata, M. Gen, Cellular genetic algorithm for multi-objective optimization, in: Proceedings of the 4th Asian Fuzzy System Symposium, Citeseer, 2002, pp. 538–542.

[13] Q. Zhang, H. Li, MOEA/D: a multiobjective evolutionary algorithm based on decomposition, IEEE Transactions on Evolutionary Computation. 11 (6) (2007) 712–731.

[14] H. L. Liu, F. Gu, Q. Zhang, Decomposition of a multiobjective optimization problem into a number of simple multiobjective subproblems, IEEE Transactions on Evolutionary Computation. 18 (3) (2014) 450–455.

[15] K. Li, K. Deb, Q. Zhang, S. Kwong, An evolutionary many-objective optimization algorithm based on dominance and decomposition, IEEE Transactions on Evolutionary Computation. 19 (5) (2015) 694–716.

[16] M. Li, S. Yang, X. Liu, Pareto or Non-Pareto: bi-criterion evolution in multiobjective optimization, IEEE Transactions on Evolutionary Computation. 20 (5) (2016) 645–665.

[17] Y. Liu, D. Gong, J. Sun, Y. Jin, A many-objective evolutionary algorithm using a one-by-one selection strategy, IEEE Transactions on Cybernatics. (accepted).

[18] M. Fleischer, The measure of Pareto optima applications to multi-objective metaheuristics, in: Proceedings of the Evolutionary Multi-criterion Optimization, Springer, 2003, pp. 519–533.

[19] E. Zitzler, L. Thiele, Multiobjective evolutionary algorithms: a comparative case study and the strength Pareto approach, IEEE Transactions on Evolutionary Computation. 3 (4) (1999) 257–271.

[20] N. Beume, B. Naujoks, M. Emmerich, SMS-EMOA: multiobjective selection based on dominated hypervolume, European Journal of Operational Research 181 (3) (2007) 1653–1669.

[21] J. Bader, E. Zitzler, HypE: an algorithm for fast hypervolume-based many-objective optimization, Evolutionary Computation 19 (1) (2011) 45–76.

[22] H. Wang, L. Jiao, X. Yao, Two_Arch2: an improved two-archive algorithm for many-objective optimization, IEEE Transactions on Evolutionary Computation. 19 (4) (2015) 524–541.

[23] C. A. Rodríguez Villalobos, C. A. C. Coello, A new multi-objective evolutionary algorithm based on a performance assessment indicator, in: Proceedings of the Genetic and Evolutionary Computation Conference, ACM, 2012, pp. 505–512.

[24] H. Ishibuchi, H. Masuda, Y. Tanigaki, Y. Nojima, Modified distance calculation in generational distance and inverted generational distance., in: EMO (2), 2015, pp. 110–125.

[25] E. M. Lopez, C. A. C. Coello, Improving the integration of the IGD+ indicator into the selection mechanism of a multi-objective evolutionary algorithm, in: Evolutionary Computation (CEC), 2017 IEEE Congress on, IEEE, 2017, pp. 2683–2690.

[26] O. Schutze, X. Esquivel, A. Lara, C. A. C. Coello, Using the averaged hausdorff distance as a performance measure in evolutionary multiobjective optimization, IEEE Transactions on Evolutionary Computation. 16 (4) (2012) 504–522.

[27] D. Brockhoff, T. Wagner, H. Trautmann, R2 indicator-based multiobjective search, Evolutionary Computation 23 (3) (2015) 369–395.

[28] M. P. Hansen, A. Jaszkiewicz, Evaluating the quality of approximations to the non-dominated set, IMM, Department of Mathematical Modelling, Technical Universityof Denmark, 1998.

[29] H. Trautmann, T. Wagner, D. Brockhoff, R2-EMOA: focused multiobjective search using R2-indicator-based selection, in: International Conference on Learning and Intelligent Optimization, Springer, 2013, pp. 70–74.

[30] R. H. Gómez, C. A. C. Coello, MOMBI: a new metaheuristic for many-objective optimization based on the R2 indicator, in: Proceedings of IEEE Congress on Evolutionary Computation, 2013, pp. 2488–2495.

[31] D. H. Phan, J. Suzuki, R2-BEAN: R2 indicator based evolutionary algorithm for noisy multiobjective optimization, in: the 2014 Seventh IEEE Symposium on Computational Intelligence for Security and Defense Applications, 2014, pp. 1–8.

[32] F. Li, J. Liu, S. Tan, X. Yu, R2-MOPSO: a multi-objective particle swarm optimizer based on R2-indicator and decomposition, in: Proceedings of IEEE Congress on Evolutionary Computation, IEEE, 2015, pp. 3148–3155.

[33] J. G. Falcón-Cardona, C. A. C. Coello, A new indicator-based many-objective ant colony optimizer for continuous search spaces, Swarm Intelligence 11 (1) (2017) 71–100.

[34] Y. Tan, Y. Jiao, H. Li, X. Wang, MOEA/D + uniform design: a new version of MOEA/D for optimization problems with many objectives, Computers and Operations Research 40 (6) (2013) 1648 – 1660.

[35] B. Derbel, D. Brockhoff, A. Liefooghe, S. Verel, On the impact of multi-objective scalarizing functions, in: Parallel Problem Solving from Nature–PPSN XIII, Springer, 2014, pp. 548–558.

[36] R. H. Gómez, C. A. C. Coello, Improved metaheuristic based on the R2 indicator for many-objective optimization, in: Proceedings of the Genetic and Evolutionary Computation Conference, ACM, 2015, pp. 679–686.

[37] M. Asafuddoula, T. Ray, R. Sarker, A decomposition-based evolutionary algorithm for many objective optimization, IEEE Transactions on Evolutionary Computation. 19 (3) (2015) 445–460.

[38] R. Cheng, Y. Jin, M. Olhofer, B. Sendhoff, A reference vector guided evolutionary algorithm for many-objective optimization, IEEE Transactions on Evolutionary Computation. 20 (5) (2016) 773–791.

[39] D. H. Phan, J. Suzuki, R2-IBEA: R2 indicator based evolutionary algorithm for multiobjective optimization, in: Proceedings of the IEEE Congress on Evolutionary Computation, IEEE, 2013, pp. 1836–1845.

[40] K. Miettinen, Nonlinear multiobjective optimization, volume 12 of international series in operations research and management science (1999).

[41] K. Deb, R. B. Agrawal, Simulated binary crossover for continuous search space, Complex Systems 9 (3) (1994) 1–15.

[42] K. Deb, M. Goyal, A combined genetic adaptive search (geneas) for engineering design, Computer Science and Informatics 26 (1996) 30–45.

[43] J. A. Cornell, Experiments with mixtures: designs, models, and the analysis of mixture data, Vol. 895, John Wiley & Sons, 2011.

[44] K. Deb, L. Thiele, M. Laumanns, E. Zitzler, Scalable multi-objective optimization test problems, in: Proceedings of the IEEE Congress on Evolutionary Computation, Vol. 1, IEEE, 2002, pp. 825–830.

[45] S. Huband, P. Hingston, L. Barone, L. While, A review of multiobjective test problems and a scalable test problem toolkit, IEEE Transactions on Evolutionary Computation. 10 (5) (2006) 477–506.

[46] Y. Tian, R. Cheng, X. Zhang, Y. Jin, PlatEMO: a matlab platform for evolutionary multi-objective optimization, arXiv preprint arXiv:1701.00879.

[47] M. Hollander, D. A. Wolfe, E. Chicken, Nonparametric statistical methods, John Wiley & Sons, 2013.

[48] Y. Wang, B. C. Wang, H. X. Li, G. G. Yen, Incorporating objective function information into the feasibility rule for constrained evolutionary optimization, IEEE Transactions on Cybernetics. pp (99) (2015) 1–15.

[49] R. Cheng, Y. Jin, M. Olhofer, B. Sendhoff, Test problems for large-scale multiobjective and many-objective optimization, IEEE Transactions on Cybernetics. pp (99) (2016) 1–14.